

23	Table of contents	
24	Text S1 Characterization of DOM chemical property and molecular composition....	S3
25	Text S2 Characterization of EDC and Fe(II) contents of pot experiment soils	S4
26	Text S3 16S rRNA gene sequencing	S5
27	Text S4 Rice grain element contents	S7
28	Text S5 DOM mediated <i>Shewanella oneidensis</i> MR-1 reduction of ferrihydrite.....	S8
29	Text S6 Fitting method	S9
30	Text S7 Pot soil microbial community dynamics	S12
31	Table S1 Physicochemical properties of As-contaminated paddy soil.....	S13
32	Table S2 Physicochemical properties of AC and RC	S14
33	Table S3 Alpha diversity indicators of soil microbial community.....	S15
34	Table S4 Criteria for molecular formula classification of FTICR-MS data	S16
35	Figure S1 Second-year un-filling rice grain and harvested ratoon rice.....	S17
36	Figure S2 Original soil Fe(III) reduction and As release.....	S18
37	Figure S3 Original soil EDC and correlation analysis.....	S19
38	Figure S4 Fitting rates in all microcosm incubations	S20
39	Figure S5 Pot-incubated soils Fe(III) reduction and As release	S21
40	Figure S6 Pot-incubated soils EDC and correlation analysis	S22
41	Figure S7 Co-occurrence of Fe(II) and methane in microcosm incubations.....	S23

42	Figure S8 First-year pot soil EDC and Fe(II) content.....	S24
43	Figure S9 First-year and second-year pot experiments porewater pH	S25
44	Figure S10 Pot soil microbial community composition	S26
45	Figure S11 Three fluorescent components in EEM-PARAFAC models	S27
46	Figure S12 Molecular-level FT-ICR MS analysis of DOM	S28
47	Figure S13 Tannins and lignins molecular weight distribution	S29
48	Figure S14 EEM spectra of DOM before and after AC/RC adsorption.....	S30
49	Figure S15 Calculated porewater DOM quinone content	S31
50	Figure S16 EEM spectra of DOM in AC and lactate co-amended soils	S32
51	Figure S17 Symptom of straight-head disease	S33
52	Figure S18 First-year rice grain and husk trace and nutrient elements content	S34
53	Figure S19 Second-year rice grain and husk trace and nutrient elements content ...	S35
54	Figure S20 First-year pot porewater dissolved sulfate concentrations.....	S36
55	Figure S21 First-year pot upper layer porewater chemistry	S37

56

57 **Text S1 Characterization of DOM chemical property and molecular composition**

58 The concentration of dissolved organic carbon (DOC) in porewater of soil
59 microcosms and pot experiments were measured using a total organic carbon analyzer
60 (Vario TOC cube, Elementar, Germany). The absorption spectra of the samples were

61 measured using a UV-Vis spectrophotometer (Cary 60, Agilent). Fluorescence
62 emission-excitation matrix (EEM) spectra of porewater were recorded using a Hitachi
63 F-7000 spectrofluorometer (Tokyo, Japan) with excitation wavelengths of 200-550 nm
64 at 5 nm intervals and emission wavelengths of 250-600 nm at 2 nm intervals. The
65 fluorescence intensity was then normalized using the Raman scattering peak of water
66 to Raman units. The fluorescence spectra of porewater were analyzed using the EEM-
67 PARAFAC model in MATLAB R2021b using the DOMFLuor toolbox.¹

68 The porewater dissolved organic matter (DOM) molecular composition was
69 determined using Fourier-transform ion cyclotron resonance mass spectrometry (FT-
70 ICR MS) and analyzed using the in-house Matlab script TRFu. DOM was extracted
71 from the porewater of the three treatments using solid phase extraction (SPE).² FTICR-
72 MS spectra were measured by a Bruker Solarix mass spectrometer (Bruker, Germany)
73 equipped with a 15.0 T superconducting magnet with electrospray ionization (ESI) in
74 negative ion mode, with m/z from 100 to 1600 Da. The molecular formula classification
75 of FT-ICR MS data was listed in Table S4 below.³

Text S2 Characterization of electronic donating capacity (EDC) and Fe(II) content of pot experiment soils

At 137 d of the first-year pot experiment, upper layer (3-7 cm) and lower layer (13-17 cm) soils were sampled from the pots and transferred into the glovebox within a few seconds. Three 1.00 g subsamples were weighted into 15 mL centrifuge tubes. Then, 10 mL of 1 M HCl, 10 mL of 6 M HCl, and 10 mL of ferricyanide solutions (10 mM potassium ferricyanide, 3 M NaCl, and 100 mM phosphate buffer) were sequentially spiked into the centrifuge tubes, which were then transferred in a glovebox. After 5, 6, and 24 h of reaction in the glovebox, the samples were analyzed to quantify the low-crystalline Fe(II) and Fe(III) content, high-crystalline Fe(II) and Fe(III) content, and electron-donating capacity of these pot soils, respectively. Afterward, the supernatant samples were taken out and filtered using a 0.22 μ m membrane filter. The filtrates were measured spectrophotometrically at 510 nm and 420 nm as soon as possible to determine the Fe(II)/Fe(III) content and electron accumulation capacity of the soils, respectively.^{4, 5}. The rest of the soil was dried to determine water content of the soils.

Text S3 16S rRNA gene amplicon sequencing and data analysis

During the two-year pot experiments, the soil samples were collected at 40, 75, and 120 d in the first-year and 131 d in the second-year and storage in a -80°C refrigerator. The soil FastDNA Spin Kit (MP Biomedicals, USA) was used to extract soil DNA. PCR amplification of the bacterial 16S rRNA genes V3–V4 region was performed using the forward primer 338F (5'-ACTCCTACGGGAGGCAGCA-3') and the reverse primer 806R (5'-GGACTACHVGGGTWTCTAAT-3'). Sample-specific 7-bp barcodes were incorporated into the primers for multiplex sequencing. The PCR components contained 5 µL of buffer (5×), 0.25 µL of Fast pfu DNA Polymerase (5U/µL), 2 µL (2.5 mM) of dNTPs, 1 µL (10 µM) of each Forward and Reverse primer, 1 µL of DNA Template, and 14.75 µL of H₂O. Thermal cycling consisted of initial denaturation at 98°C for 2 min, followed by 25 cycles consisting of denaturation at 98°C for 15 s, annealing at 55°C for 30 s, and extension at 72°C for 30 s, with a final extension of 5 min at 72°C. PCR amplicons were purified with Vazyme V AHTSTM DNA Clean Beads (Vazyme, Nanjing, China) and quantified using the Quant-iT PicoGreen dsDNA Assay Kit (Invitrogen, Carlsbad, CA, USA). After the individual quantification step, amplicons were pooled in equal amounts, and pair-end 2×250 bp sequencing was performed using the Illumina NovaSeq platform with NovaSeq 6000 SP Reagent Kit (500 cycles) at Shanghai Personal Biotechnology Co., Ltd (Shanghai, China).

Sequence data analyses were mainly performed using QIIME2 and R packages (v3.2.0). ASV-level alpha diversity indices, including Chao1, observed species, Phylogenetic diversity (PD) Whole Tree Shannon index, and Simpson index were calculated using the ASV table in QIIME2. ASV-level ranked abundance curves were generated to compare the richness and evenness of ASVs among samples. Beta diversity analysis was performed to investigate the structural variation of microbial communities across samples using Jaccard metrics,⁶ Bray-Curtis metrics,⁷ and UniFrac distance metrics,^{8,9} as well as visualized via nonmetric multidimensional scaling (NMDS) and unweighted pair-group method with arithmetic means (UPGMA) hierarchical clustering.¹⁰ The raw sequence data are deposited in the National Genomics Data Center (NGDC) (<https://ngdc.cncb.ac.cn/gsa>) (GSA: CRA015577).

Text S4 Analysis of total As and some nutrients and trace elements concentration and arsenic speciation in rice grains.

Powdered subsamples (0.1 g) of over-dried grain samples were digested with 5 mL of high-purity concentrated HNO₃ using a graphite digestion device.^{11, 12} Total As and some nutrients and trace elements (P, Fe, Cd, Mn, Zn, Cu, and Ca) in grain and husk was determined by inductively coupled plasma–mass spectrometry (ICP-MS, PerkinElmer NexION 2000). The 1% HNO₃ acid extraction method was used to extract arsenic speciation in rice grains.¹³ In brief, powdered subsamples (0.2g) were weighed and extracted with 10 mL of 1% high-purity HNO₃. Gradient from room temperature to 75 °C with holding times of 10 min, then to 95 °C with holding times of 30 min. After digestion, the extracts were centrifuged at 3214g for 10min and filtered through a 0.22 µm membrane. As species in grain were separated and analyzed using high-performance liquid chromatography–inductively coupled plasma–mass spectrometry (HPLC-ICP-MS, PerkinElmer NexION 2000). Chromatographic separations were performed using a commonly used HPLC system with an anion exchange column. A Hamilton PRP-X100 column (length, 250mm; diameter, 4.1mm) was used with an isocratic phosphate / nitrate eluent (15mM NH₄H₂PO₄ and 15 mM NH₄NO₃, pH 6.0) and a flow rate of 1.0 mL min⁻¹.¹²

Text S5 *Shewanella oneidensis* MR-1 reduction of ferrihydrite experiment

Preparation of ferrihydrite. Ferrihydrite was synthesized using the method described by Amstaetter et al.¹⁴ The synthesized product was washed with ultrapure water and suspended in ultrapure water to achieve a concentration of 200 mM Fe(III). The suspension was then deoxygenated by stirring and N₂ purging for 2 hours. Finally, the suspension was stored in the dark in serum bottles sealed with a thick butyl rubber stopper and aluminum crimp.¹⁵

Microbial cultivation. A pure culture of *Shewanella oneidensis* MR-1 (ATCC No. 700550) was aerobically cultured in Luria-Bertani medium under temperature-controlled conditions (28°C, 150 rpm) for 14-16 hours. The cells were harvested by centrifugation at 7000 rpm for 5 min, washed with anoxic bicarbonate buffer (30 mM, pH 7.0), and re-suspended at a density of approximately 2×10^{11} cells mL⁻¹.¹⁵

Text S6 Fitting method

CO₂ and CH₄ accumulation in soil microcosm incubations.

We used these concentrations to determine total concentrations of CO₂ or CH₄ in the gas and aqueous phase ($C_{CO_2,CH_4,total,t}$) per gram of soil at each sampling point t using Eq. 1.

$$C_{CO_2,CH_4,total,t} = \frac{n_{CO_2,CH_4,(g),t} + n_{CO_2,CH_4,(aq),t}}{DW} \quad (1)$$

where $n_{CO_2,CH_4,(g),t}$, and $n_{CO_2,CH_4,(aq),t}$ are the moles of CO₂ or CH₄ in the gas and aqueous phase, respectively, at time t , and DW is the dry weight of the soil.

The value of $n_{CO_2,CH_4,(g),t}$ was determined directly from the measured concentration of CO₂ or CH₄ ($C_{CO_2,CH_4,(g),t}$, in ppmv) following Eq. 2.

$$n_{CO_2,CH_4,(g),t} = \frac{C_{CO_2,CH_4,(g),t} \times 10^{-6} \times V_{headspace,t}}{V_m} \quad (2)$$

where $V_{headspace}$ is the headspace volume in the reactor and is equal to 63.5 mL. V_m is molar volume of gas and is equal to 24.7 L mol⁻¹ at 28 °C, and 1.01×10⁵Pa. Note that the factor 10⁻⁶ reflects the transformation of ppmv to volume fraction.

We assumed the gas and liquid phase to be in equilibrium and determined $n_{CO_2,CH_4,(aq),t}$ using Henry's law Eq. 3.

$$n_{CO_2,CH_4,(aq),t} = C_{CO_2,CH_4,(g),t} \times 10^{-6} \times K_H \times V_{suspension,t} \quad (3)$$

where $C_{CO_2,CH_4,(g),t} \times 10^{-6}$ is the partial pressure of CO₂ or CH₄ at time t (in atm), assuming partial pressure equals volume fraction times experimental pressure of 1 atm, and K_H is the Henry constant for CO₂ (0.0341 mol L⁻¹ atm⁻¹)¹⁶ or CH₄ (0.0015 M mol L⁻¹ atm⁻¹)¹⁶ at experimental conditions of 1 atm pressure and 298 K. The cumulative

concentration of CO₂ or CH₄ produced until time t was calculated by adding concentrations at time t to cumulative concentrations at the preceding sampling point.¹⁷

Fe(III) reduction rate in soil microcosm incubations. Logistic and exponential models were used to simulate the relationship between Fe(II) accumulation and incubation time in each treatment by Origin 2023. The logistic model can be expressed as:

$$Y_t = \frac{a}{1 + b \times e^{-ct}} \quad (4)$$

where, Y_t is the Fe(II) concentration measured after incubation for t (d); and a , b , and c are the parameters in this formula. The derivative of Y_t is:

$$V = \frac{dY_t}{dt} = Y_t \times c \times \left(1 - \frac{Y_t}{a}\right) \quad (5)$$

The derivative of V is:

$$\frac{dV}{dt} = \frac{d}{dt} \left(\frac{dY_t}{dt} \right) = Y_t \times c^2 \times \left(1 - \frac{3Y_t}{a} + \frac{2Y_t^2}{a^2}\right) \quad (6)$$

when the derivative of V is zero, it means that the Fe(III) reduction rate reaches the maximum. Then the value for Y_t can be calculated according to Eq. 6 and is equal to $0.5a$. The value for Y_t can be used in Eq. 5 to obtain V_{\max} , which is equal to $0.25ac$.¹⁸

The Fe(III) reduction rate in the manuscript refers to V_{\max} .

Electron accumulation rate in soil microcosm incubations. The method to fit the electron accumulation rate is the same as the method used for fitting the iron reduction rate. The electron accumulation rate in the manuscript refers to V_{\max} .

CO₂ emission rate in soil microcosm incubations. To obtain CO₂ emission rate,

we fit CO₂ accumulation to Eq. 7 by Origin 2023, which normalized to dry soil grams ($C_{CO_2,cum,t}$).

$$C_{CO_2,cum,t} = a \times (1 - e^{-bt}) \quad (7)$$

where a and b are parameters optimized in the fit and t is time. The parameters a and b were subsequently used in the derivative of the above function to calculate initial CO₂ emission rate at t = 1 d ($R_{CO_2,t=1d}$) according to Eq. 8.¹⁷

$$R_{CO_2,t} = a \times b \times e^{-bt} \quad (8)$$

The CO₂ emission rate in the manuscript refers to initial CO₂ emission rate at t = 1 d.

As release rate in soil microcosm incubations. As release rate in soil microcosm incubations was obtained by linear regression from the steepest slopes of the As release curve.

Ferrihydrite reduction rate in *Shewanella oneidensis* MR-1 incubations.

Ferrihydrite reduction rate in pure culture incubations was acquired by linear regression from the steepest slopes of the Fe(II) accumulation curve.

Text S7 Pot soil microbial community dynamics

Insignificant change of alpha diversity indexes among different treatments at different rice growth stages demonstrated AC and RC amendments did not affect community richness, community diversity, and phylogenetic diversity (Table S3, SI). Insignificant differences were observed for AC, RC and CK treatments at the phylum level (Fig. S10a, SI). Bacterial community in CK treatment closely associated with RC treatment but obviously separated from AC treatment (Fig. S10b, SI). But further taxonomical classification at the genus level revealed few significant changes in potential Fe(III) reducers (Fig. S10c, SI). These results demonstrated the decreased porewater DOM in AC treatment did not significantly alter microbial growth but possibly affect microbial metabolic activities. Biochar insignificantly impacts flooding paddy soil microbial community composition has also been reported previously.^{19, 20}

221 **Table S1 Physicochemical properties of the arsenic contaminated paddy soil**

Soil characteristics	Values
pH	5.72
TOC (g kg ⁻¹)	22.2
CEC (cmol kg ⁻¹)	13.6
Total P (mg kg ⁻¹)	841
Total Fe (g kg ⁻¹)	35.8
Total As (mg kg ⁻¹)	29.3
Total Cd (mg kg ⁻¹)	0.35
Total Mn (mg kg ⁻¹)	214
Soil texture	Silty clay loam

222 Note: cation-exchange capacity (CEC).

223 **Table S2 The BET, elemental composition, and electron donating and accepting capacities (EDC and EAC) of activated carbon (AC)**

224 **and rice straw biochar (RC)**

	pH	BET surface area (m ² g ⁻¹)	C (wt.%)	O (wt.%)	H (wt.%)	N (wt.%)	EDC (mmol e ⁻ g ⁻¹)	EAC (mmol e ⁻ g ⁻¹)
AC	7.05	871.0	82.15	3.708	0.939	0.47	0.069	1.41
RC	9.89	15.7	67.71	7.61	2.178	1.44	0.070	0.844

225

226 **Table S3 Diversity indicators (α -diversity) of soil microbial communities in the lower layer of pot experiment**

Time (d)	Treatment	Chao1	Observed species	PD whole tree	Shannon	Simpson
40d (1)	CK	2847 \pm 153a	2691 \pm 148a	264.6 \pm 26.3a	10.24 \pm 0.08a	0.9982 \pm 0.0001a
	AC	3029 \pm 26a	2882 \pm 33a	246.6 \pm 14.1a	10.41 \pm 0.07a	0.9985 \pm 0.0002a
	RC	2870 \pm 99a	2727 \pm 96a	285.7 \pm 43.1a	10.20 \pm 0.15a	0.9980 \pm 0.0005a
75d (1)	CK	2916 \pm 102a	2727 \pm 101a	286.0 \pm 74.6a	10.24 \pm 0.05a	0.9982 \pm 0.0000a
	AC	2936 \pm 126a	2792 \pm 98a	324.8 \pm 59.6a	10.31 \pm 0.11a	0.9981 \pm 0.0004a
	RC	2840 \pm 209a	2703 \pm 179a	288.1 \pm 50.0a	10.18 \pm 0.08a	0.9976 \pm 0.0003a
120d (1)	CK	2834 \pm 150a	2703 \pm 130a	238.1 \pm 20.7a	10.27 \pm 0.03a	0.9982 \pm 0.0002a
	AC	2886 \pm 230a	2747 \pm 211a	286.3 \pm 78.2a	10.33 \pm 0.14a	0.9983 \pm 0.0002a
	RC	2986 \pm 174a	2861 \pm 137a	303.1 \pm 41.4a	10.25 \pm 0.1a	0.9979 \pm 0.0004a
135d (2)	CK	2779 \pm 144b	2690 \pm 141b	282.4 \pm 20.4ab	10.28 \pm 0.12a	0.9981 \pm 0.0004a
	AC	2714 \pm 64b	2630 \pm 65b	244.8 \pm 27.0b	10.27 \pm 0.02a	0.9982 \pm 0.0000a
	RC	3018 \pm 96a	2944 \pm 94a	320.0 \pm 33.6a	10.42 \pm 0.17a	0.9984 \pm 0.0005a

227 Five α -diversity indices: Chao1, Observed species, and Phylogenetic diversity (PD) Whole Tree, Shannon index and Simpson index. (Duncan's

228 multiple range test at $p < 0.05$, data are means \pm SD (n = 3)) The first-year paddy soil label bore "(1)" and the second year label bore "(2)".

229 **Table S4 Criteria for molecular formula classification of FT-ICR MS data**

Molecular class	Criteria
Carbohydrate	H/C:1.5-2.4;O/C:0.71-1.2
Amino sugars	H/C:1.5-2.2;O/C:0.52-0.71
Protein/lipid-like	H/C:1.5-2.2;O/C:0-0.52
Tannins	H/C:0.5-1.5;O/C:0.67-1.2
Lignins/carboxyl-rich acyclic molecules	H/C:0.7-1.5;O/C:0.1-0.67
Unsaturated hydrocarbons	H/C:0.8-1.5;O/C:0-0.1
Condensed aromatic structures	H/C:0.3-0.7;O/C:0-0.67

230



Figure S1 Second-year un-filling rice grain and harvested ratoon rice. Symptoms of un-filling rice grain (upper left) and harvested ratoon rice (upper right) from the second-year pot experiment. The cutting panicles (lower picture).

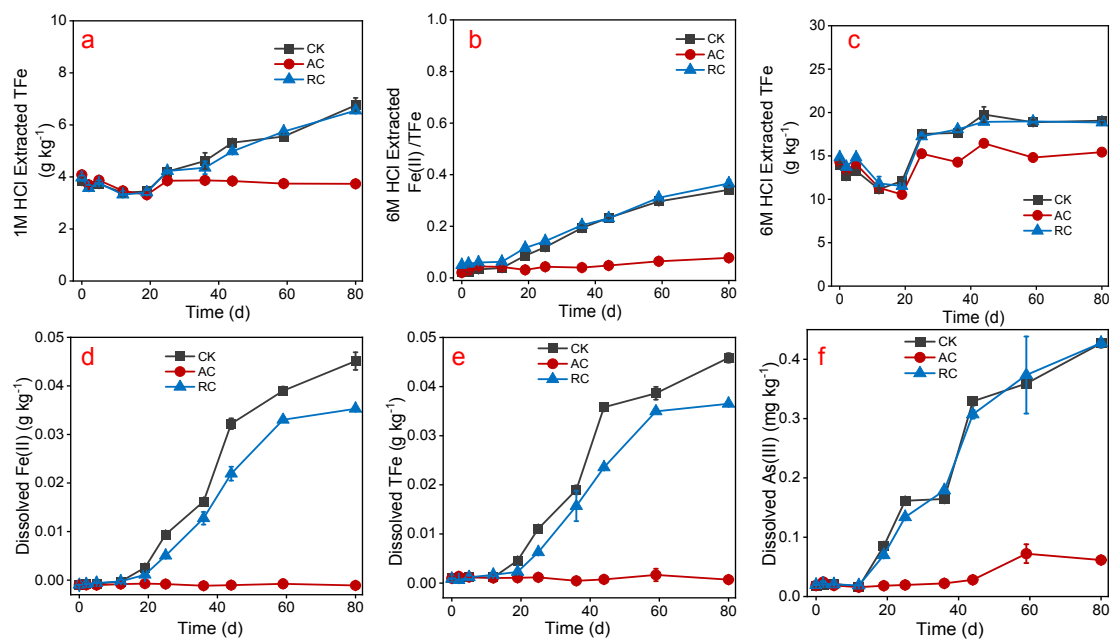


Figure S2 Original soil Fe(III) reduction and As release. Microcosm incubation for original paddy soils. The 1 M HCl extracted total Fe (a), 6 M HCl extracted Fe(II) to total Fe ratio (b), 6M HCl extracted total Fe (c), dissolved Fe²⁺ (d), dissolved total Fe (e), and dissolved arsenite (As(III), f) during the original soil microcosm incubation. The extracted total Fe and dissolved As have been normalized to dry soil weight. The error bars represent the standard deviations between duplicate experiments (n = 2).

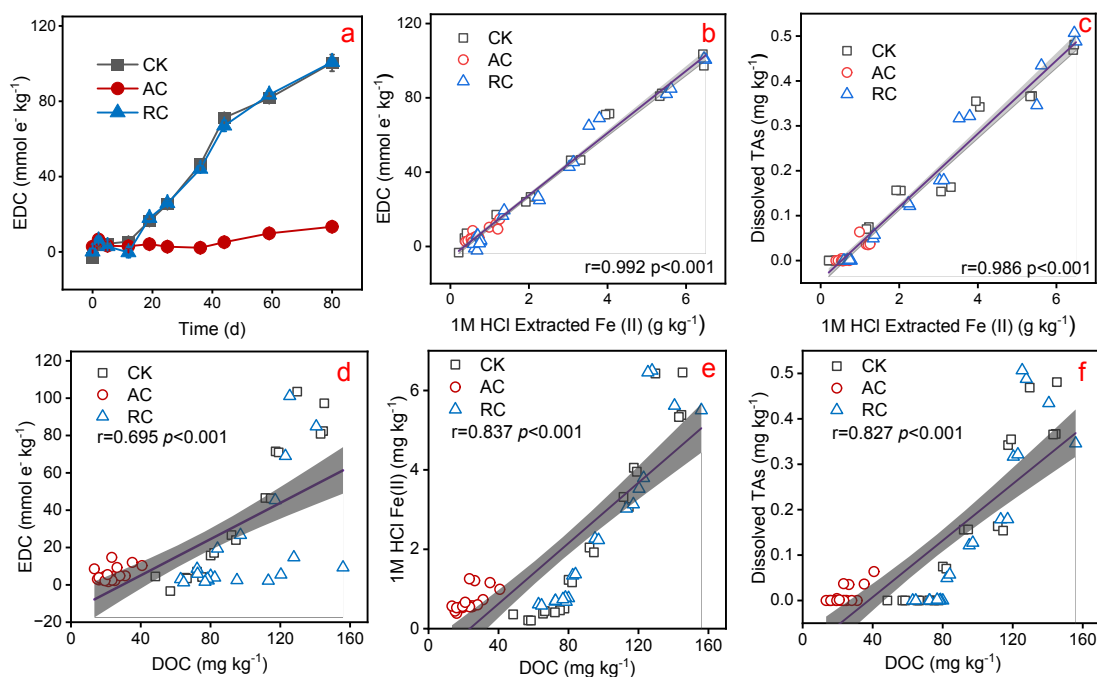


Figure S3 Original soil EDC and correlation analysis. Electron-donating capacity (EDC) of activated carbon (AC) or rice straw biochar (RC) or not (CK) amended original paddy soils during microcosm incubation. Correlation analysis of 1M HCl extracted Fe(II) with EDC (b) or dissolved arsenic (As, c). Correlation analysis of dissolved organic carbon (DOC) with EDC (d) or 1M HCl extracted Fe(II) (e) or dissolved As (f). The gray areas in the figure represent 95% confidence interval. The error bars represent the standard deviations between duplicate experiments (n = 2).

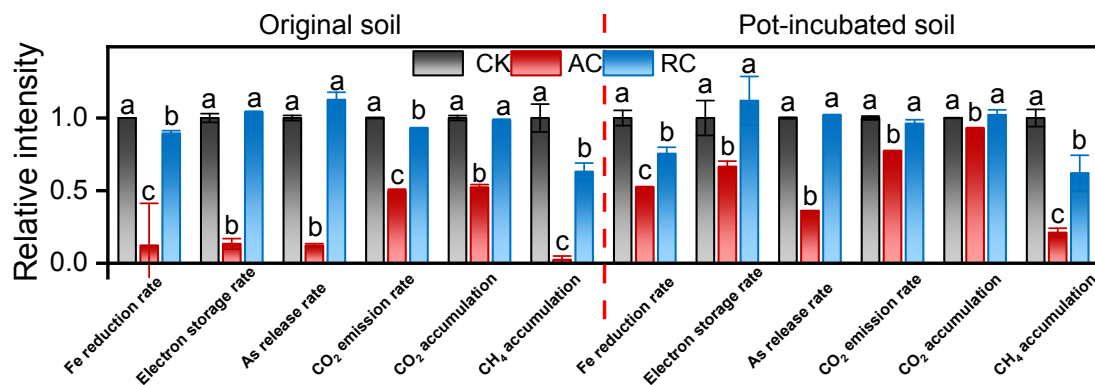


Figure S4 Fitting rates in all microcosm incubations. Relative intensities of Fe(III) reduction rate, electron accumulation rate, As release rate, CO₂ emission rate, CO₂ accumulation, and CH₄ accumulation in the AC and RC treatments compared to the CK treatment in the original soils and the pot-incubated soils microcosm incubations. Different letters indicate significant difference at $p < 0.05$ according to Duncan's test. The error bars represent the standard deviations between duplicate experiments ($n = 2$).

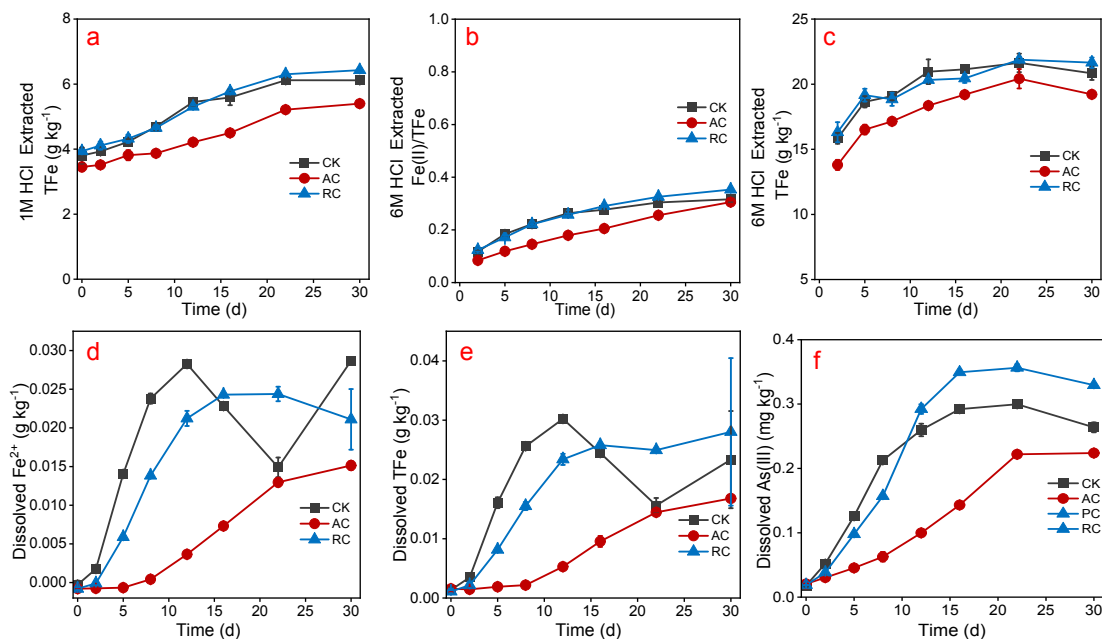


Figure S5 Pot-incubated soils Fe(III) reduction and As release. Microcosm incubation for pot-incubated soils collected from the pot at 76 d in the second-year pot experiment. The 1 M HCl extracted total Fe (a), 6 M HCl extracted Fe(II) to total Fe ratio (b), 6 M HCl extracted total Fe (c), dissolved Fe^{2+} (d), dissolved total Fe (e), and dissolved arsenite (As(III), f) during the pot-incubated soils microcosm incubation. The extracted total Fe and dissolved As has been normalized to dry soil weight. The error bars represent the standard deviations between duplicate experiments ($n = 2$).

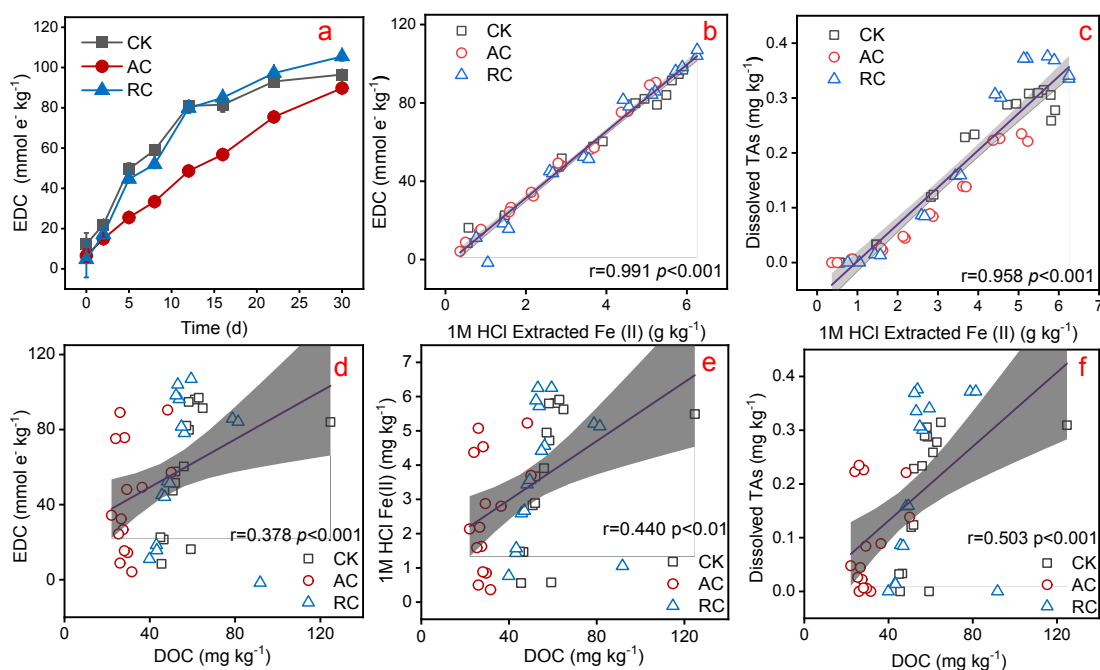


Figure S6 Pot-incubated soils EDC and correlation analysis. Electron-donating capacity (EDC) of activated carbon (AC) or rice straw biochar (RC) or not (CK) amended pot-incubated soils (collected from the pot at 76 d in the second-year pot experiment) during microcosm incubation. Correlation analysis of 1M HCl extracted Fe(II) with EDC (b) or dissolved arsenic (As, c). Correlation analysis of dissolved organic carbon (DOC) with EDC (d) or 1M HCl extracted Fe(II) (e) or dissolved As (f). The gray areas in the figure represent 95% confidence interval. The error bars represent the standard deviations between duplicate experiments (n = 2).

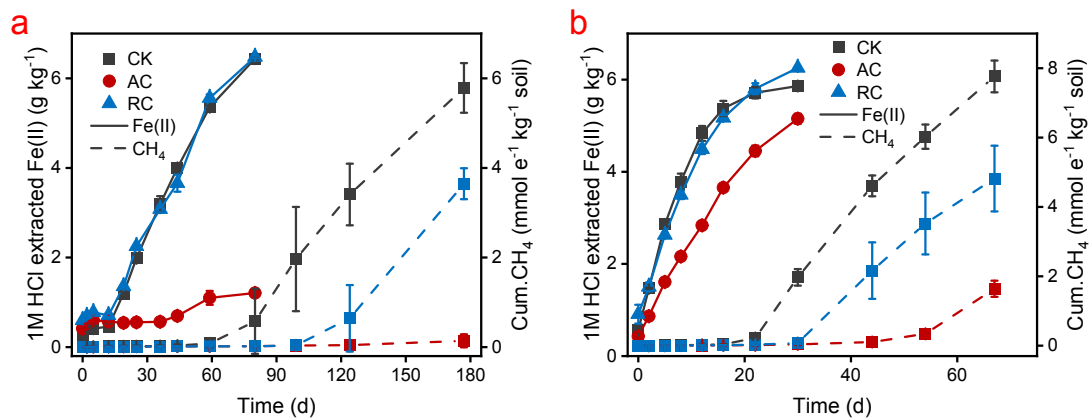


Figure S7 Co-occurrence of Fe(II) and methane in microcosm incubations. The co-occurrence of Fe(II) and methane during the original soils (a) and pot-incubated soils (b) microcosm incubations. The error bars represent the standard deviations between duplicate experiments (n = 2).

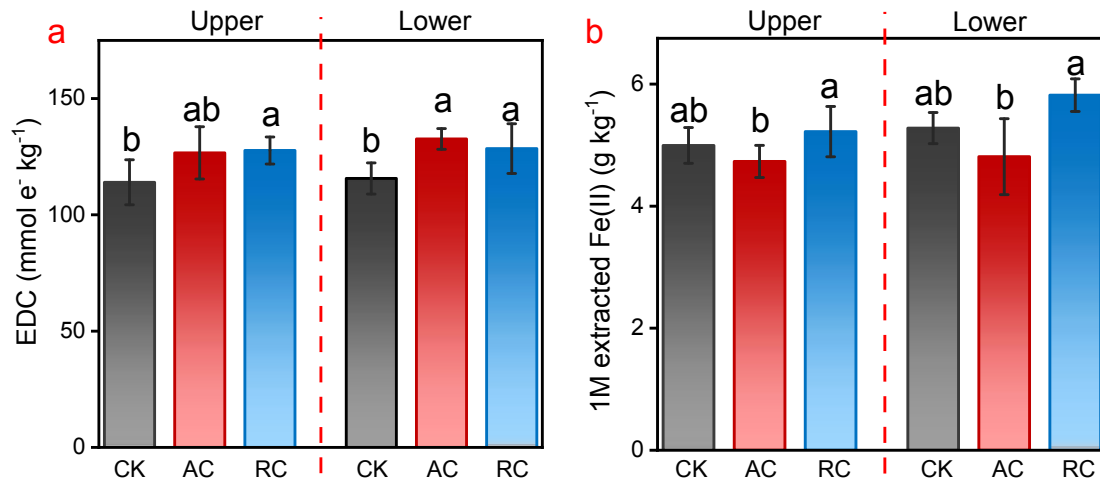


Figure S8 First-year pot soil EDC and Fe(II) content. Electron donating capacity (EDC, a) and Fe(II) content (b) of upper and lower layer soils collected from the pots at 137 d during the first-year pot experiment. At this sampling time, the full flooding soils were able to produce methane. Data are means \pm SD ($n = 6$). Different letters indicate significant difference at $p < 0.05$ according to Duncan's test.

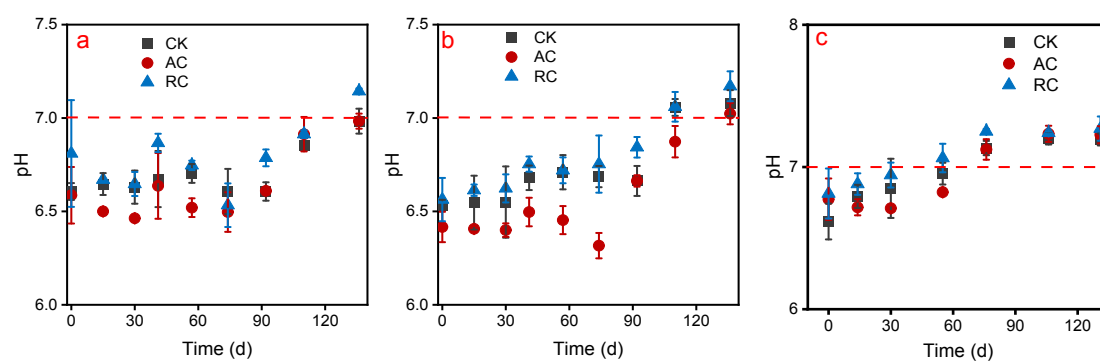
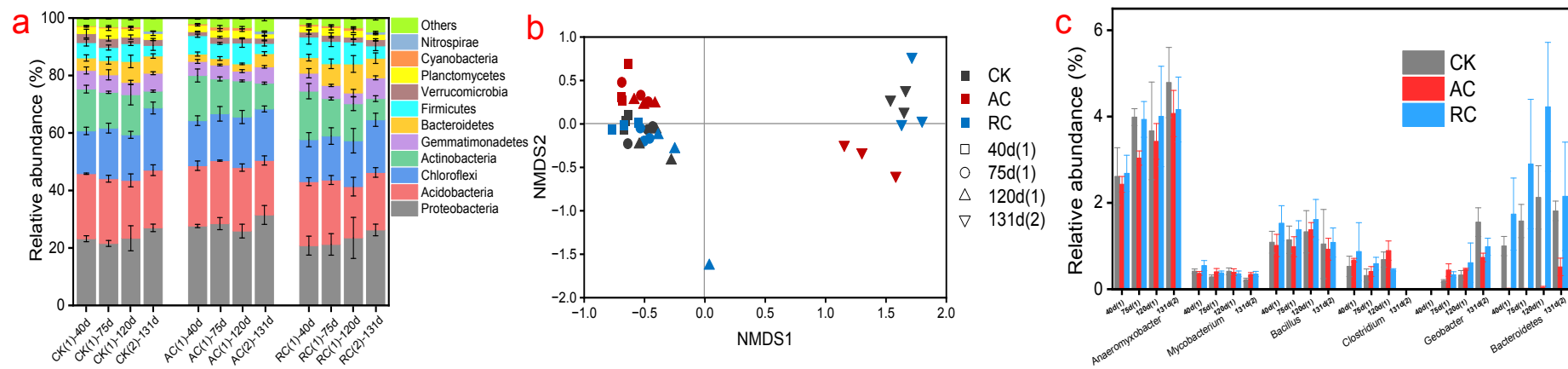


Figure S9 First-year and second-year pot experiments porewater pH. Porewater pH of lower layer (a and c) and upper layer (b) during the first-year (a and b) and second-year (c) pot experiments. The error bars represent the standard deviations between triplicate experiments ($n = 3$).



291

292 **Figure S10 Pot soil microbial community composition.** Lower layer soil microbial community dynamics during the two-year pot experiments

293 with the amendment of activated carbon (AC) or rice straw biochar (RC) or untreated (CK) at different rice growth stages. Relative abundance of

294 potential active bacteria at phylum level (a), (b) Non-metric multidimensional scaling (NMDS) analysis of microbial communities (β -diversity, b),

295 relative abundance of Fe(III)-reducing bacteria (c). The symbols (1) and (2) behind time referred to first-year and second-year pot soils, respectively.

296 The error bars represent the standard deviations between triplicate experiments ($n = 3$).

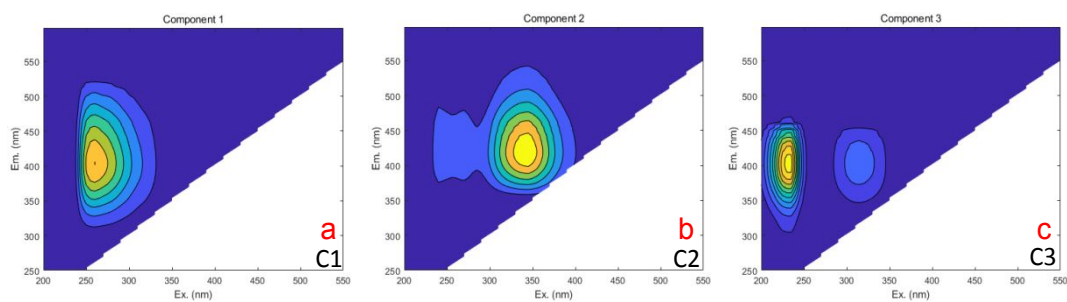


Figure S11 Three fluorescent components in EEM-PARAFAC models. Three split-half validated fluorescent humic-like (C1, a), UVC humic-like (C2, b), and UVA humic-like (C3, c) components of EEM-PARAFAC models using EEM spectroscopy. Porewater dissolved organic matter collected at different rice growth stages during two-year pot experiments were analyzed.

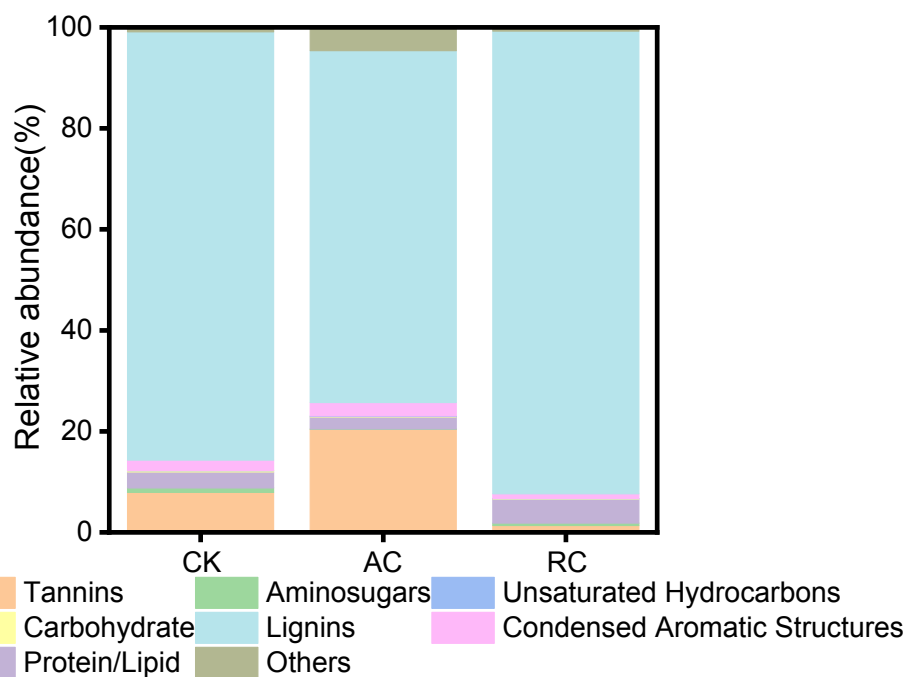


Figure S12 Molecular-level FT-ICR MS analysis of DOM. Molecular-level FT-ICR MS analysis of dissolved organic matter (DOM): Porewater DOM composition bar plots. The porewater was sampled from pot at 76 d during second-year pot experiment.

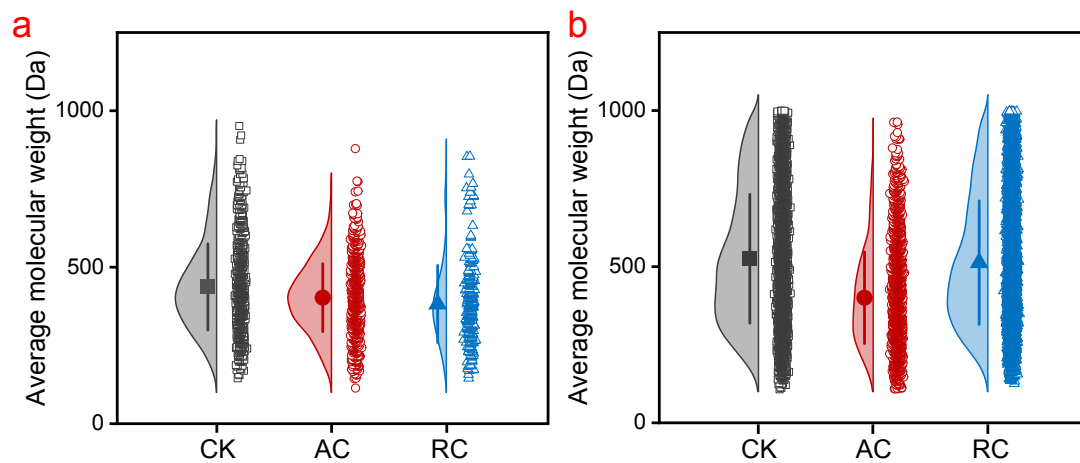


Figure S13 Tannins and lignins molecular weight distribution. Tannins (a) and lignins (b) molecular weight distribution acquired from FT-ICR MS analysis result.

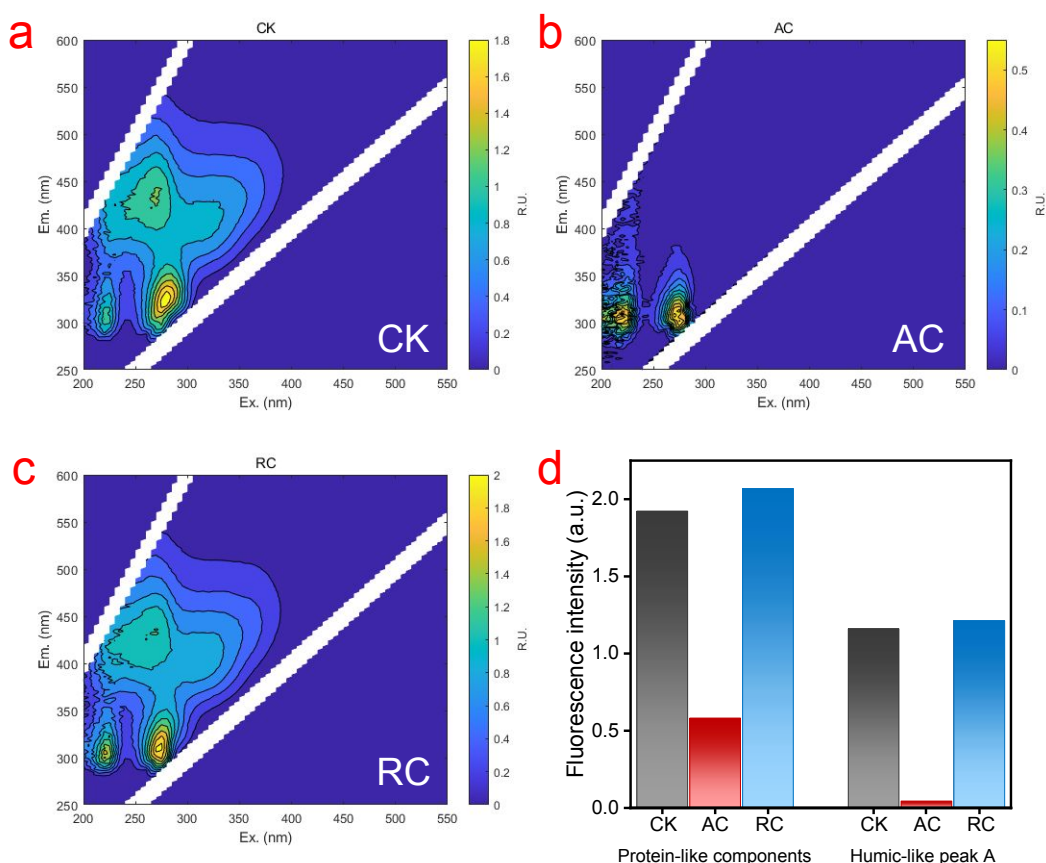


Figure S14 EEM spectra of DOM before and after AC/RC adsorption. Emission-excitation matrix spectra characterization of soil extracted DOM fluorescent property with AC/RC amended. Ten grams soil was mixed with 20 mL Milli-Q water and shaken for 30 min to extract DOM. AC and RC (2 g L^{-1}) were added to the DOM solution and shaken for 1 h. The resultant supernatant was filtered and collected for EEM characterization: soil extracted DOM (a), supernatant after AC adsorption (b), and supernatant after RC adsorption (c). The fluorescence intensity of protein-like components and humic-like peak A in three treatments was shown in the bar plots (d).

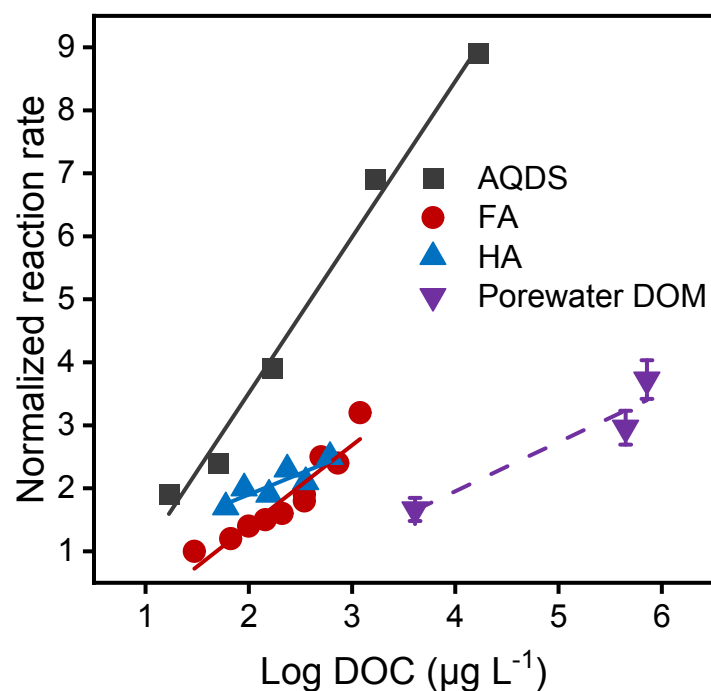


Figure S15 Calculated porewater DOM quinone content. Normalized Fe(III) reduction rates in response to different content of electron shuttles, including porewater DOM, AQDS, groundwater humic acid (HA), and groundwater fluvic acid (FA). Normalized Fe(III) reduction rate was calculated from the electron shuttle mediated microbial Fe(III) reduction kinetic result. Porewater DOM related data were performed in this study. AQDS, HA, and FA related data were acquired from Wolf et al. study.²¹ Linear fitting slopes for porewater DOM, AQDS, HA, and FA mediated microbial Fe(III) reduction were 0.777, 2.48, 0.669, and 1.28, respectively. Accordingly, porewater DOM quinone content was approximately one-third of that in AQDS, with a value of 0.024 mol quinone/mol C.

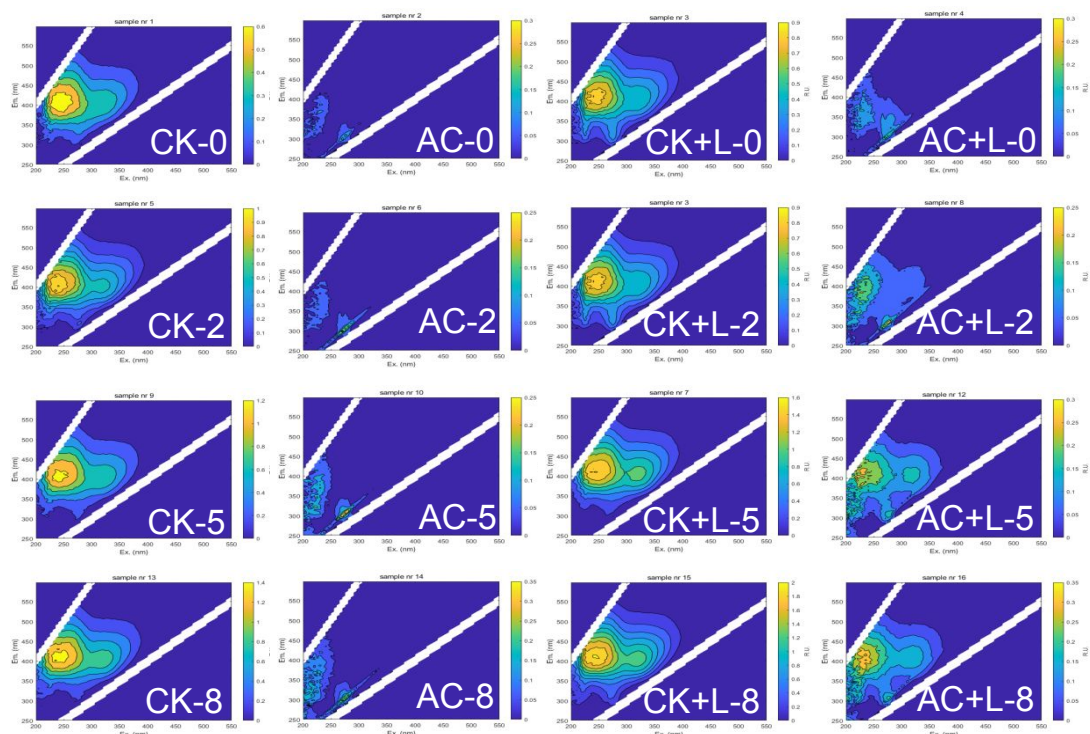


Figure S16 EEM spectra of DOM in AC and lactate co-amended soils. Emission-excitation matrix spectra characterization of solution phase dissolved organic matter fluorescent property during activated carbon (AC) and sodium lactate co-amendment soil microcosm incubations. Four treatments were included: only soil (CK), amend AC (AC), amend sodium lactate (CK+L), and amend AC and sodium lactate (AC+L). The number after CK-, AC-, CK+L-, and AC+L- referred to sampling times of 0, 2, 5, and 8 d. Fluorescence intensities were normalized to Raman units using the Raman scatter peak of water.



Figure S17 Symptom of straight-head disease. Symptoms of straight-head disease of rice harvested from the control treatment pots in the first-year pot experiment (upper pictures). Upper right picture is a zoom-in look of the left picture. Lower pictures show the harvested rice panicles from representative CK, AC, and RC treatment pots.

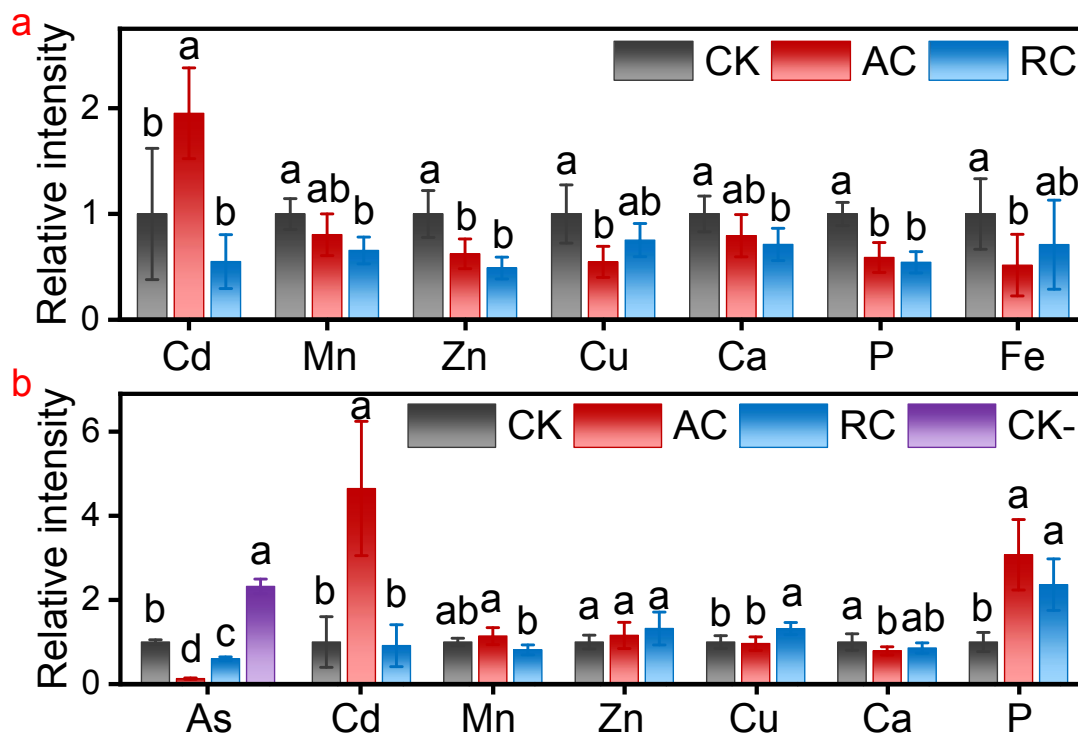


Figure S18 First-year rice grain and husk trace and nutrient elements content.

Relative content (normalized to CK) of trace (As, Cd, Mn, Zn, Cu,) and nutritional elements (Ca, P, and Fe) in the rice grain (a) and husk (b) during the first-year pot experiment with the application of activated carbon (AC) or rice straw biochar (RC) or untreated (CK). The CK- referred to unground husk due to straight disease in the CK treatment. Data are means \pm SD (n = 6). Different letters indicate significant difference at $p < 0.05$ according to Duncan's test. Noting the significant higher content of Cd in grain and husk was possibly caused by the inhibited sulfate reduction with the application of AC.

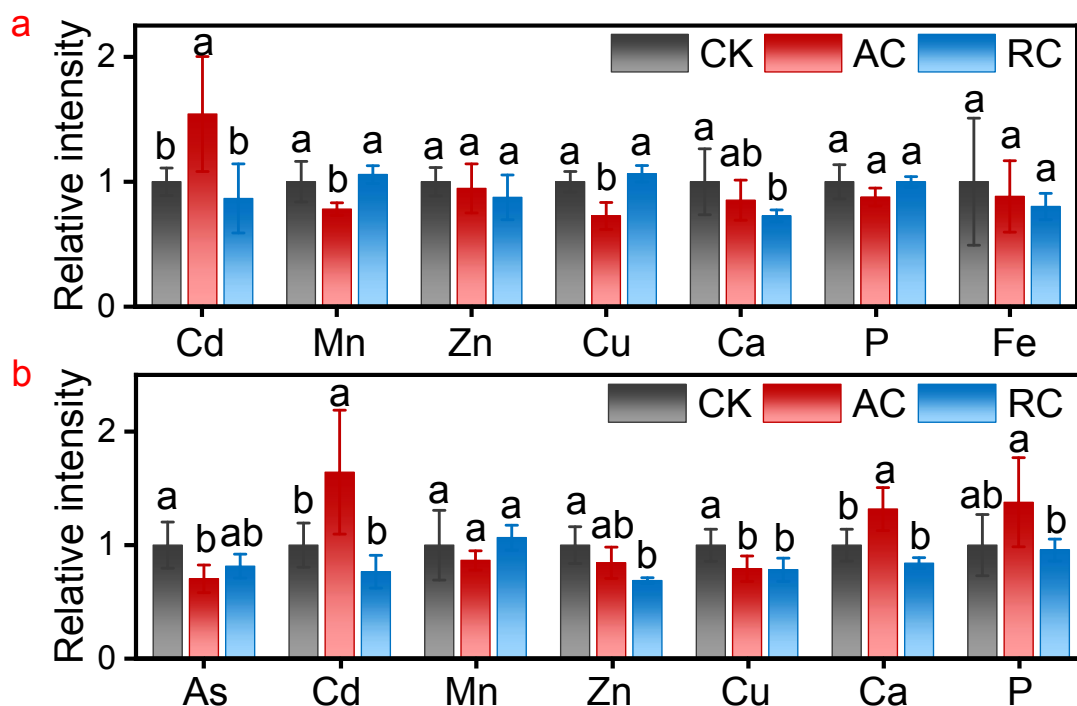


Figure S19 Second-year rice grain and husk trace and nutrient elements content.

Relative content (normalized to CK) of trace (As, Cd, Mn, Zn, Cu,) and nutritional elements (Ca, P, and Fe) in the rice grain (a) and husk (b) during the second-year pot experiment with the application of activated carbon (AC) or rice straw biochar (RC) or untreated (CK). Data are means \pm SD (n = 6). Different letters indicate significant difference at $p < 0.05$ according to Duncan's test. Noting the significant higher content of Cd in grain and husk was possibly caused by the inhibited sulfate reduction with the application of AC.

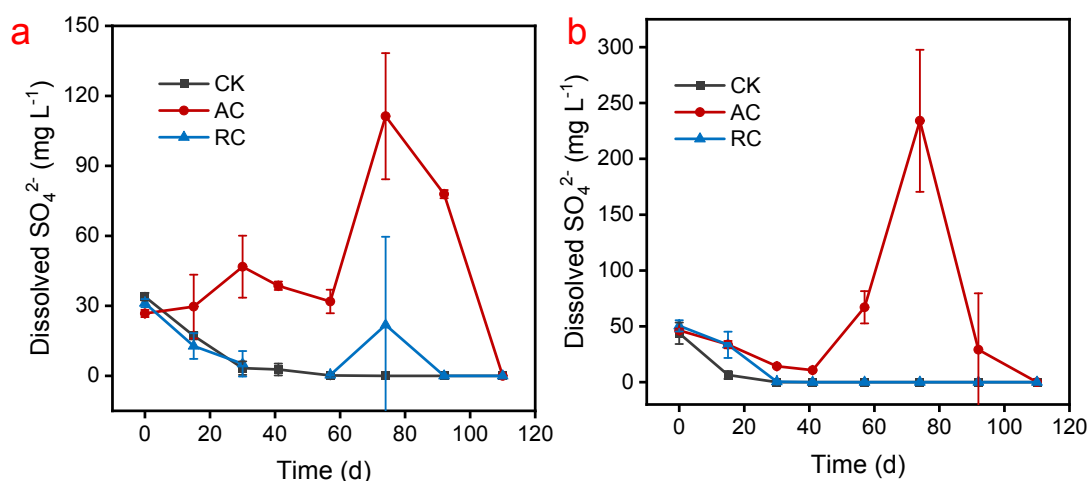


Figure S20 First-year pot porewater dissolved sulfate concentrations. Porewater dissolved SO_4^{2-} concentration in upper (a) and lower (b) layer porewater during first-year pot experiment with the application of activated carbon (AC) or rice straw biochar (RC) or untreated (CK). The error bars represent the standard deviations between triplicate experiments (n = 3).

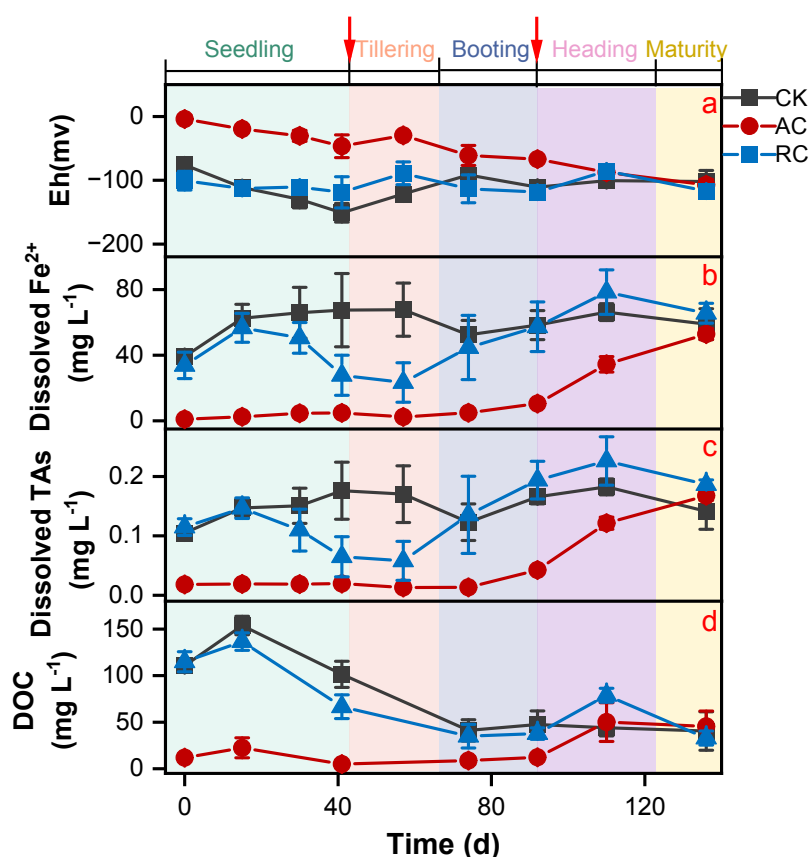


Figure S21 First-year pot upper layer porewater chemistry. Upper layer porewater redox potential (Eh, a), dissolved Fe²⁺ (b), dissolved arsenic (As, c), and dissolved organic carbon (DOC, d) concentrations during the first-year pot experiment with the application of activated carbon (AC) or rice straw biochar (RC) or untreated (CK). Rice growth is divided into seeding, tillering, booting, heading, and maturity stages. Red arrows indicate the application of nitrogen fertilizer. The error bars represent the standard deviations between triplicate experiments (n = 3).

References

1. Stedmon, C. A.; Bro, R., Characterizing dissolved organic matter fluorescence with parallel factor analysis: a tutorial. *Limnol. Oceanogr.: Methods* **2008**, *6*, (11), 572-579.
2. Dittmar, T.; Koch, B.; Hertkorn, N.; Kattner, G., A simple and efficient method for the solid-phase extraction of dissolved organic matter (SPE-DOM) from seawater. *Limnol. Oceanogr.: Methods* **2008**, *6*, (6), 230-235.
3. Fu, Q. L.; Fujii, M.; Riedel, T., Development and comparison of formula assignment algorithms for ultrahigh-resolution mass spectra of natural organic matter. *Anal. Chim. Acta* **2020**, *1125*, 247-257.
4. Sun, T.; Guzman, J. J.; Seward, J. D.; Enders, A.; Yavitt, J. B.; Lehmann, J.; Angenent, L. T., Suppressing peatland methane production by electron snorkeling through pyrogenic carbon in controlled laboratory incubations. *Nat. Commun.* **2021**, *12*, (1), 4119.
5. Xin, D.; Xian, M.; Chiu, P. C., New methods for assessing electron storage capacity and redox reversibility of biochar. *Chemosphere* **2019**, *215*, 827-834.
6. Jaccard, P., Nouvelles recherches sur la distribution florale. *Bull. Soc. Vaud. Sci. Nat.* **1908**, *44*, 223-270.
7. Bray, J. R.; Curtis, J. T., An ordination of the upland forest communities of southern Wisconsin. *Ecol. Monogr.* **1957**, *27*, (4), 326-349.
8. Lozupone, C.; Knight, R., UniFrac: a new phylogenetic method for comparing microbial communities. *Appl. Environ. Microbiol.* **2005**, *71*, (12), 8228-35.
9. Lozupone, C. A.; Hamady, M.; Kelley, S. T.; Knight, R., Quantitative and qualitative β diversity measures lead to different insights into factors that structure microbial communities. *Appl. Environ. Microbiol.* **2007**, *73*, (5), 1576-1585.
10. Ramette, A., Multivariate analyses in microbial ecology. *FEMS Microbiol. Ecol.* **2007**, *62*, (2), 142-60.
11. Zarcinas, B.; Cartwright, B.; Spouncer, L., Nitric acid digestion and multi-element analysis of plant material by inductively coupled plasma spectrometry. *Commun. Soil Sci. Plant Anal.* **1987**, *18*, (1), 131-146.
12. Dai, J.; Tang, Z.; Gao, A.-X.; Planer-Friedrich, B.; Kopittke, P. M.; Zhao, F.-J.; Wang, P., Widespread occurrence of the highly toxic dimethylated monothioarsenate (DMMTA) in rice globally. *Environ. Sci. Technol.* **2022**, *56*, (6), 3575-3586.
13. Zhu, Y.-G.; Sun, G.-X.; Lei, M.; Teng, M.; Liu, Y.-X.; Chen, N.-C.; Wang, L.-H.; Carey, A.; Deacon, C.; Raab, A., High percentage inorganic arsenic content of mining impacted and nonimpacted Chinese rice. *Environ. Sci. Technol.* **2008**, *42*, (13), 5008-5013.
14. Amstaetter, K.; Borch, T.; Kappler, A., Influence of humic acid imposed changes of ferrihydrite aggregation on microbial Fe (III) reduction. *Geochim. Cosmochim. Acta* **2012**, *85*, 326-341.
15. Wu, S.; Fang, G.; Wang, Y.; Zheng, Y.; Wang, C.; Zhao, F.; Jaisi, D. P.; Zhou, D., Redox-active oxygen-containing functional groups in activated carbon facilitate microbial reduction of ferrihydrite. *Environ. Sci. Technol.* **2017**, *51*, (17), 9709-9717.
16. Sander, R., Compilation of Henry's law constants (version 4.0) for water as solvent. *Atmospheric Chem. Phys* **2015**, *15*, (8), 4399-4981.

17. Aeppli, M.; Thompson, A.; Dewey, C.; Fendorf, S., Redox Properties of Solid Phase Electron Acceptors Affect Anaerobic Microbial Respiration under Oxygen-Limited Conditions in Floodplain Soils. *Environ. Sci. Technol.* **2022**, *56*, (23), 17462-17470.
18. Jiangzhou, H.; Dong, Q., Dissimilatory Fe (III) reduction characteristics of paddy soil extract cultures treated with glucose or fatty acids. *J. Environ. Sci.* **2008**, *20*, (9), 1103-1108.
19. Wang, N.; Xue, X. M.; Juhasz, A. L.; Chang, Z. Z.; Li, H. B., Biochar increases arsenic release from an anaerobic paddy soil due to enhanced microbial reduction of iron and arsenic. *Environ. Pollut.* **2017**, *220*, 514-522.
20. Tian, J.; Wang, J.; Dippold, M.; Gao, Y.; Blagodatskaya, E.; Kuzyakov, Y., Biochar affects soil organic matter cycling and microbial functions but does not alter microbial community structure in a paddy soil. *Sci. Total Environ.* **2016**, *556*, 89-97.
21. Wolf, M.; Kappler, A.; Jiang, J.; Meckenstock, R. U., Effects of humic substances and quinones at low concentrations on ferrihydrite reduction by *Geobacter metallireducens*. *Environ. Sci. Technol.* **2009**, *43*, (15), 5679-5685.